Chapter 21
Experimental Nonlinear Vibration Analysis of a Shrouded Bladed Disk Model on a Rotating Test Rig

Ferhat Kaptan, Lars Panning-von Scheidt, and Jörg Wallaschek

Abstract The optimization of the mechanical design process of turbomachinery has already been subject of research for decades. In this context, many researchers developed efficient numerical methods to calculate the vibration response of bladed disks. In particular, shrouded bladed disks with frictional contacts present a major challenge in the design process. Beside efficient simulations, the validation process plays an important role in most recent studies. The quality of the comparison depends directly on the system's boundary conditions in the simulation as well as in the experiment. For instance, the estimation of the excitation forces should be as precise as possible, because the vibration response, in particular in the nonlinear case, depends strongly on the excitation forces.

In this paper, a newly developed rotating test rig for bladed disks is introduced. The test rig consists of a rotating shaft mounted in a vacuum chamber, in order to avoid any aerodynamic loadings and damping, and an excitation with multiple permanent magnets. Here, a large number of permanent magnets is applied to approximate a continuous force distribution along the circumference. To estimate the overall force distribution, magnetic field simulations are performed and compared to the measurements with a very good agreement. Compared to other excitation methods such as a single ac-magnet or air jet excitation, the presented method manages a high energy input at a specific engine order or frequency with modest complexity. The nonlinear vibration response is measured by strain gauges for various numbers of magnets and excitation force amplitudes. The presented results are characterized by an excellent repeatability and precise measurements of resonance passages. Especially, the nonlinear behavior of the structure such as rotational speed and excitation force dependent resonance amplitudes and frequencies as well as jumping phenomena can be shown. The developed rotating test rig proves to be particularly suitable for the vibration analysis of rotating bladed disks considering nonlinearities.

Keywords Nonlinear dynamics · Bladed disk · Shroud contact · Rotating test rig

21.1 Introduction

During operation of turbomachinery, the streaming unsteady airflow causes dynamic excitation of the rotating turbine blades. Actually, the airflow is a chaotic distributed dynamic pressure field. Due to a certain number of preconnected guide vanes or other parts in the flow channel, the pressure field contains periodic components leading to a stationary harmonic excitation of the rotating system. To avoid High Cycle Fatigue (HCF) failure, a good prediction of the vibration response at the operating range of the system is necessary. Friction damping, e.g. through underplatform dampers or tip shrouds, is commonly used to reduce the vibration amplitudes by energy dissipation. The design process of friction damped blades is still subject of research due to the strongly nonlinear characteristics. The calculation of the nonlinear forced response is generally based on the well-known Multiharmonic Balance Method (MHBM)[1, 2]. Beside calculations, the experimental validation of the numerical results plays an important role in current research projects. For an accurate comparison between simulations and experiments, a clear modeling of the system's boundary conditions is required. In particular, the excitation forces have a significant influence on the force response, thus, it is essential to estimate and to predict the excitation forces as precisely as possible. Several excitation techniques are used in the literature as non-contact excitation, e.g. magnets [3, 4] or air jets [5], or piezoelectric excitation [6–9]. All methods have their benefits as well as drawbacks and depend on the specific application. For the excitation of a rotationally periodic structure, a traveling wave type excitation is necessary [10]. This can be achieved by a rotating excitation mechanism and a non-rotating test setup, and vice versa. In most studies, a so-called blisk (bladed integrated disk) without any joints is investigated to estimate for example the structural damping [6, 11] or to characterize

F. Kaptan (✉) · L. Panning-von Scheidt · J. Wallaschek
Institute of Dynamics and Vibration Research, Faculty of Mechanical Engineering, Leibniz University Hannover, Hannover, Germany
e-mail: kaptan@ids.uni-hannover.de

G. Kerschen et al. (eds.), *Nonlinear Structures and Systems, Volume 1*, Conference Proceedings of the Society for Experimental Mechanics Series, https://doi.org/10.1007/978-3-030-12391-8_21

mistuning induced mode localizations [7, 9]. Also frictionally coupled structures, for instance by underplatform dampers [3, 8], shroud contacts [12], friction rings [13] or root contacts [14], are analyzed in several studies. Due to the considerable complexity of the nonlinear vibration response of coupled rotating systems, there is still a great demand concerning this subject.

In this context, a new rotating test rig is designed and developed at the *Institute of Dynamics and Vibration Research* to measure the vibration response of bladed disks. Basically, excitation is achieved by ac-/permanent magnets, piezo patches or air jets. However, due to the high global stiffness of the investigated bladed disk model, a sufficient excitation force amplitude is needed. Thus, a large number of permanent magnets is used in this study. In particular, the blades are coupled with each other to the tip shroud and at multiple locations with the disk to the root. To analyze the nonlinear characteristics of the system, a variable excitation level is essential. Here, quasi-static ANSYS Maxwell simulations are performed and compared to an experimental setup to estimate the excitation force potential. The rotating experiments are carried out at different excitation levels in a wide rotational speed range. It should be noted that the main focus of this paper is the experimental study of a bladed disk model. However, numerical results of a linearized modal analysis will be shown in the next chapter. A detailed description of the numerical nonlinear vibration response is given in [15].

21.2 Bladed Disk Model

The investigated bladed disk model consists of 60 single blades and a comparatively rigid disk, see Fig. 21.1. The blades are statically prestressed at the tip shroud by an interference fit and coupled at multiple locations with the disk to the root. During operation, centrifugal forces cause a deformation of the system leading to a change of the contact forces. As a result, the dynamic behavior of the structure is highly nonlinear and depends on the rotational speed. To characterize the linear dynamic behavior, a numerical linear modal analysis, under the assumption of a perfectly tuned system, is applied. The symmetric properties of rotationally periodic structures can be exploited to compute the dynamic behavior of the full system by only one sector model [16]. In this study, ANSYS Mechanical is used to discretize a sector model of the system and to compute the nonlinearly prestressed cyclic modal parameters. The computational procedure is divided into two parts. First, a quasistatic nonlinear analysis is applied by considering an interference fit at the shroud contact and by preloading the structure with centrifugal forces. Subsequently, the system is linearized by considering the computed contact areas. In a second step, a modal analysis of the linearized system is applied. Here, the modal parameters, such as natural frequencies and eigenvectors, depend on the so-called nodal diameter, which corresponds to the phase relation between the cyclic edges. For instance, at

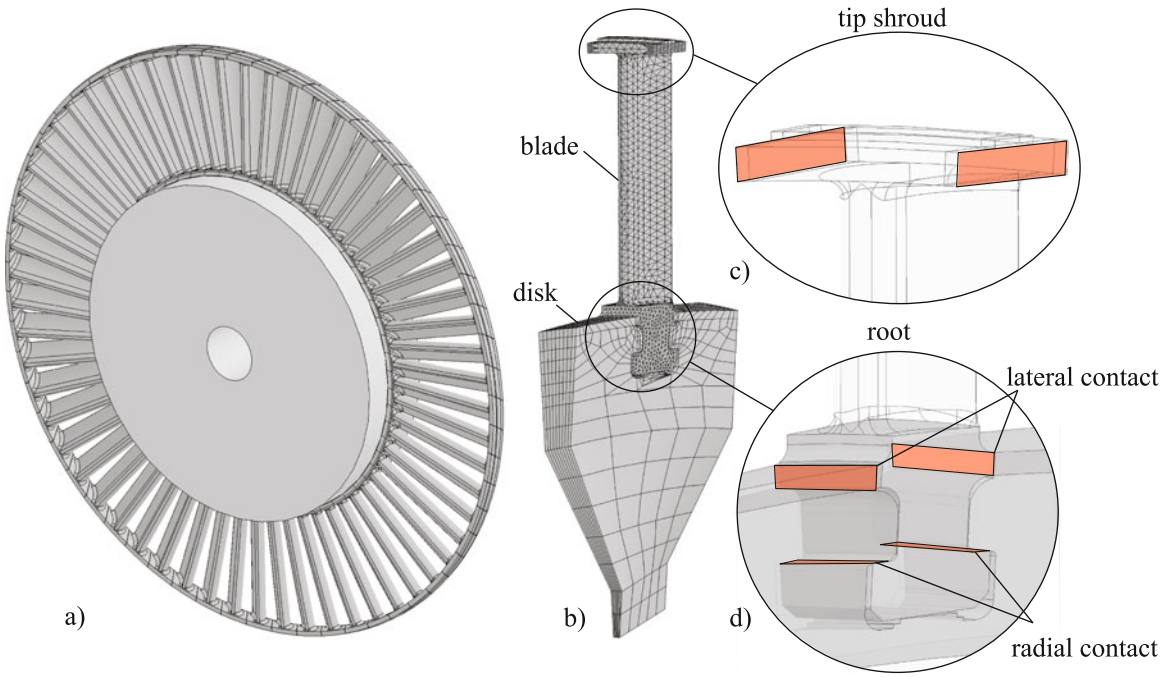

Fig. 21.1 Bladed disk model (**a**), finite element segment model (**b**), tip shroud contact area (**c**), root contact areas (**d**)

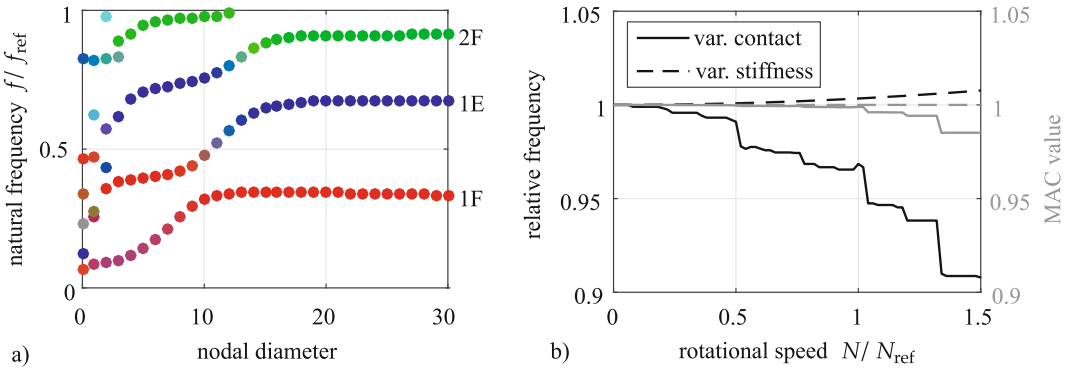

Fig. 21.2 Nodal diameter map of the linear system at zero rotational speed $N = 0$ (**a**), rotational speed dependent natural frequency and MAC value of 1F-ND15-mode (**b**)

nodal diameter zero, all blades oscillate in phase and at nodal diameter 30 (i.e. half of the amount of blades) in antiphase. The nodal diameter map is given in Fig. 21.2a at zero rotational speed. Note that the color of the dots corresponds to a mode family, i.e. red for the first flapwise (1F) mode, blue for the first edgewise (1E) mode and green for the second flapwise (2F) mode. The color scaling is based on the modal assurance criterion (MAC) value at nodal diameter 30 and illustrates nodal diameter dependent veering regions, for instance at nodal diameter 10. Veering is a well-known phenomenon regarding bladed disks, see [17]. It is caused by disk-dominated modes and, here, indicated by the color of the dots and the low correlation to the blade modes. The nodal diameter map in Fig. 21.2a is only valid for one specific rotational speed. Increasing the rotational speed leads to a change of the modal properties of the system. On the one hand, centrifugal forces increase due to the stress stiffening effect of the system's natural frequencies. On the other hand, the contact area depends on the rotational speed. To quantify the influence of both phenomena independently, the rotational speed dependent natural frequency and MAC value of the 1F-ND15-mode is shown in Fig. 21.2b. It can be seen that the natural frequency is highly sensitive to a variable contact area. The relative decrease of the natural frequency amounts to 9%, while the increase due to stress stiffening effects is approximately 1%. Regarding the MAC value, a decrease by 2% in case of a variable contact area can be noted, while a variable stiffness shows no change. Even a decrease of the MAC value by 2% is marginal, a change of the MAC value leads to a slightly different mode shape and thus to a different stress condition of the blades.

21.3 Rotating Test Rig

The experimental study is performed on the rotating test rig shown in Fig. 21.3. An electric motor is used to drive the bladed disk model up to 3600 rpm. To avoid any aerodynamic effects, such as damping or ventilation, the tests are performed in a vacuum chamber at low pressure level $p_{\text{vacuum}} < 1$ mbar. The vacuum chamber is connected to a foundation with a high mass of $m_{\text{f}} > 8$ tons and is dynamically isolated by air bearings. In addition, the vacuum chamber has several connection possibilities in radial direction and a glass window at the top of the chamber for optical measurement systems. However, in this study, strain gauges are used to measure the vibration response of the blades. The electric signals are amplified on a circuit board and transferred by a slip ring to the data acquisition. As an excitation unit, up to 45 permanent magnets are used to approximate a continuous magnetic field distribution along the circumference. A particular part of this study is the estimation of the resulting force amplitudes during operation, thus, the excitation mechanism is considered in detail in the following chapter.

21.4 Excitation Mechanism

The aim of the developed excitation unit is to excite a desired mode by a specific engine order. Due to the comparatively rigid disk and the blade coupling by shrouds, a high energy input is necessary to sufficiently excite the system. In addition, a large number of magnets is essential to excite the system at its resonance frequency in the considered rotational speed range. Regarding nonlinear systems, an accurate estimation of the excitation spectrum is particularly important. For this purpose, an ANSYS Maxwell model is set up to calculate the applying forces by magnetostatic analysis, see Fig. 21.4a. The magnetic

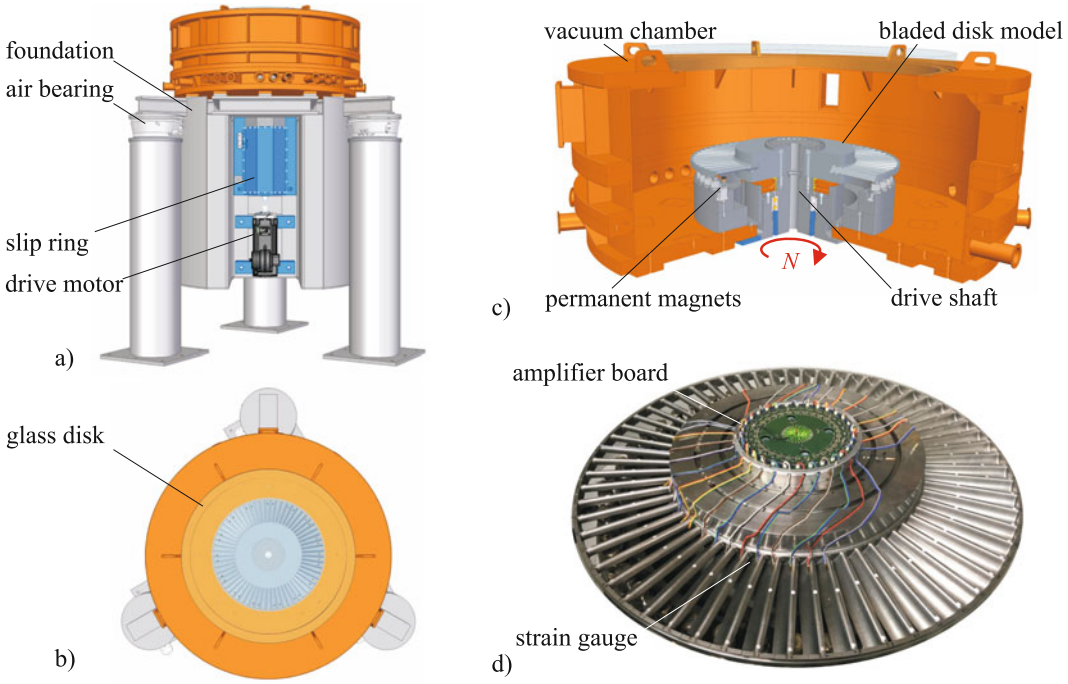

Fig. 21.3 Scheme of the rotating test rig: front view (**a**), top view (**b**), interior view (**c**), image of the bladed disk model (**d**)

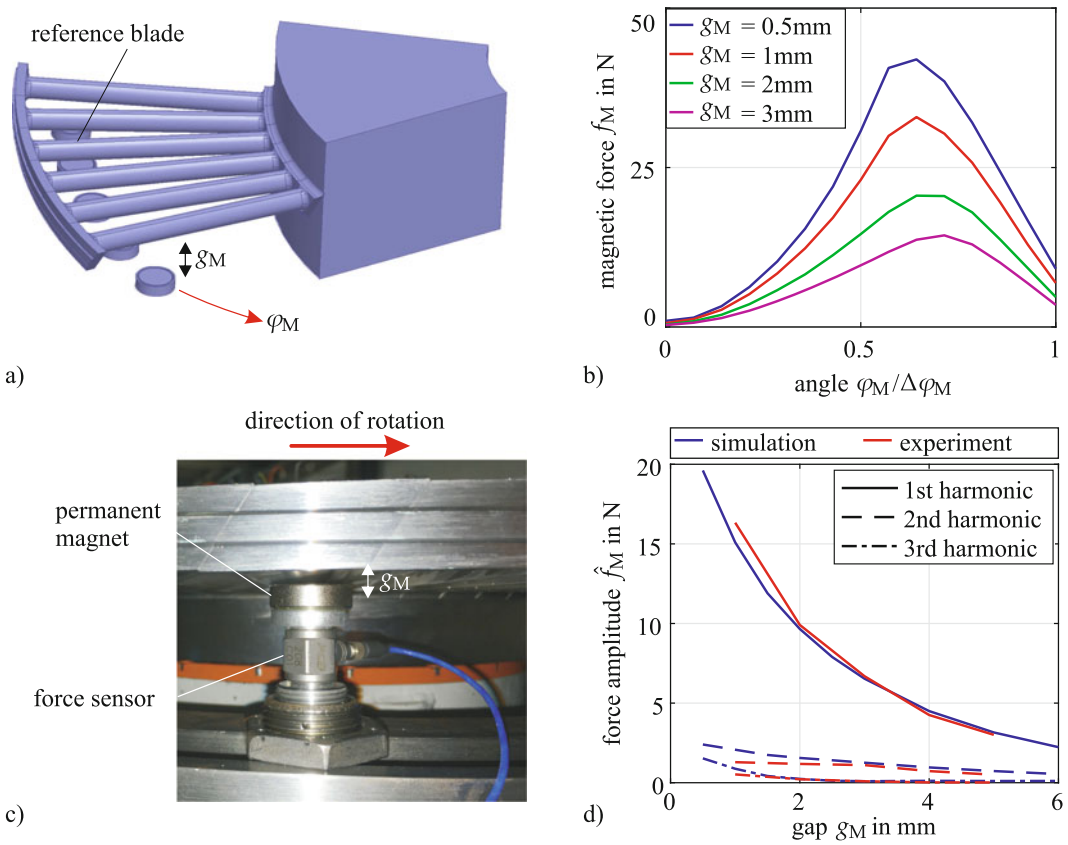

Fig. 21.4 ANSYS Maxwell simulation model (**a**), results of magnetostatic simulations (**b**), experimental setup for magnetic force measurements (**c**), comparison of simulation and experimental results (**d**)

forces are evaluated at the reference blade for various magnet gap values g_M and angles $\varphi_M/\Delta\varphi_M$, whereby $\Delta\varphi_M = 2\pi/N_M$ is defined by the number of magnets $N_M = 45$, see Fig. 21.4b. It can be noted that the static magnetic forces are highly sensitive to gap variation. The magnetic force increases up to 45 N at $g_M = 0.5$ mm and shows a sinusoidal progression over the rotation angle φ_M. However, for the rotational operation only the dynamic components of the excitation unit are crucial, which can be obtained by a decomposition of the spatial magnetic force distribution in its harmonic coefficients by FOURIER series. For the verification of the results, the magnetic forces are also measured by an experimental setup shown in Fig. 21.4c. A piezoelectric force sensor is used to measure the magnetic forces during rotation for various gap values g_M. The results of the comparison between simulation and experiment of the first three harmonic coefficients are given in Fig. 21.4d. The agreement of the comparison is remarkable. In particular, the first two harmonics are perfectly suitable for a gap variation in the rotational experiments due to a very marked gradient of the force amplitude. The third harmonic is rather unsuitable because of an approximately constant force level over the gap distance g_M. The slight deviation for $g_M < 2$ mm is caused by a mistuning of the gap between each blade and the magnet unit in the experiment. It should be noted that during the rotational experiments the magnetic forces will not be measured. To sum up, the developed permanent magnet unit is excellently suitable for the excitation of rotating bladed disks due to a high energy input in a desired engine order and an exceptional variability with respect to excitation amplitude and frequency.

21.5 Experimental Results

All measurements performed and presented in this paper are summarized in Table 21.1. The measurement series are defined by the number of magnets and by the gap value g_M. All measurements are carried out under technical vacuum conditions ($p_{vacuum} < 1$ bar) in the rotational speed range $0 \leq N \leq N_{ref}$. The vibration response is measured under steady-state conditions, meaning that the stationary vibration response of the strain gauges is recorded for each rotational speed step in the time domain. Based on this data, the mean value of the results are visualized in a Campbell diagram.

The functionality of the excitation mechanism as well as the data acquisition are investigated first. For this purpose, the Campbell diagrams of the measurement sets 1–3 are compared in Fig. 21.5. Without any magnet excitation, Fig. 21.5a, b, the structure is only excited by a dynamic imbalance of the system. Due to an adjustment of the bearings of the shaft, the imbalance of the system also has an effect in axial direction and, consequently, can excite blade modes. The vibration response shows a very low signal-to-noise ratio (SNR) but regarding the 2D Campbell diagram in Fig. 21.5b, it can clearly be seen that the response at a low order is dominant. It should be noted that the color scaling of each 2D Campbell diagram always refers to its maximum value. The rotational speed independent amplitude at $f/f\text{ref} \approx 0.8$ is caused by the cut-off frequency of the amplifier board. Considering one permanent magnet, Fig. 21.5c, the SNR is still very low, proving that a large number of magnets is necessary for the excitation of a comparatively stiff system. It is interesting to note that in this case, dominant orders can be figured out regarding the spectrum in Fig. 21.5d. Due to the 1F mode at the frequency $f/f_{ref} \approx 0.35$, see Fig. 21.2, increased amplitudes at $N/N_{ref} > 0.5$ occur. It is also notable that the spectrum shows increased amplitudes at $f/f_{ref} \approx 0.1$ over a wide rotational speed range. This frequency corresponds clearly to the system's nodal diameter 0 mode, also known as the umbrella mode, and is mainly excited by the ball pass frequency of the bearings. Increasing the number of magnets to 45, it can be recognized that the SNR significantly increases and that the engine order 45 as well as its harmonics appear mainly in the Campbell diagram, see Fig. 21.5e, f. Again, the umbrella mode appears at $f/f_{ref} \approx 0.1$, which is in this case negligible compared to the amplitudes at engine order 45 and 90. The results of the first experimental study show that the rotating test rig and, in particular, the developed excitation mechanism work as intended. In addition, the reproducibility of the measurement results is of great importance and is investigated in the following within the scope of an order analysis

Table 21.1 Overview of the measurement series

Set	Number of magnets	Gap g_M in mm	Rotational speed range
1	0	–	$0 - N_{ref}$
2	1	5	$0 - N_{ref}$
3	45	5	$0 - N_{ref}$
4	45	4	$0 - N_{ref}$
5	45	3	$0 - N_{ref}$
6	33	5	$0 - N_{ref}$
7	33	4	$0 - N_{ref}$
8	33	3	$0 - N_{ref}$

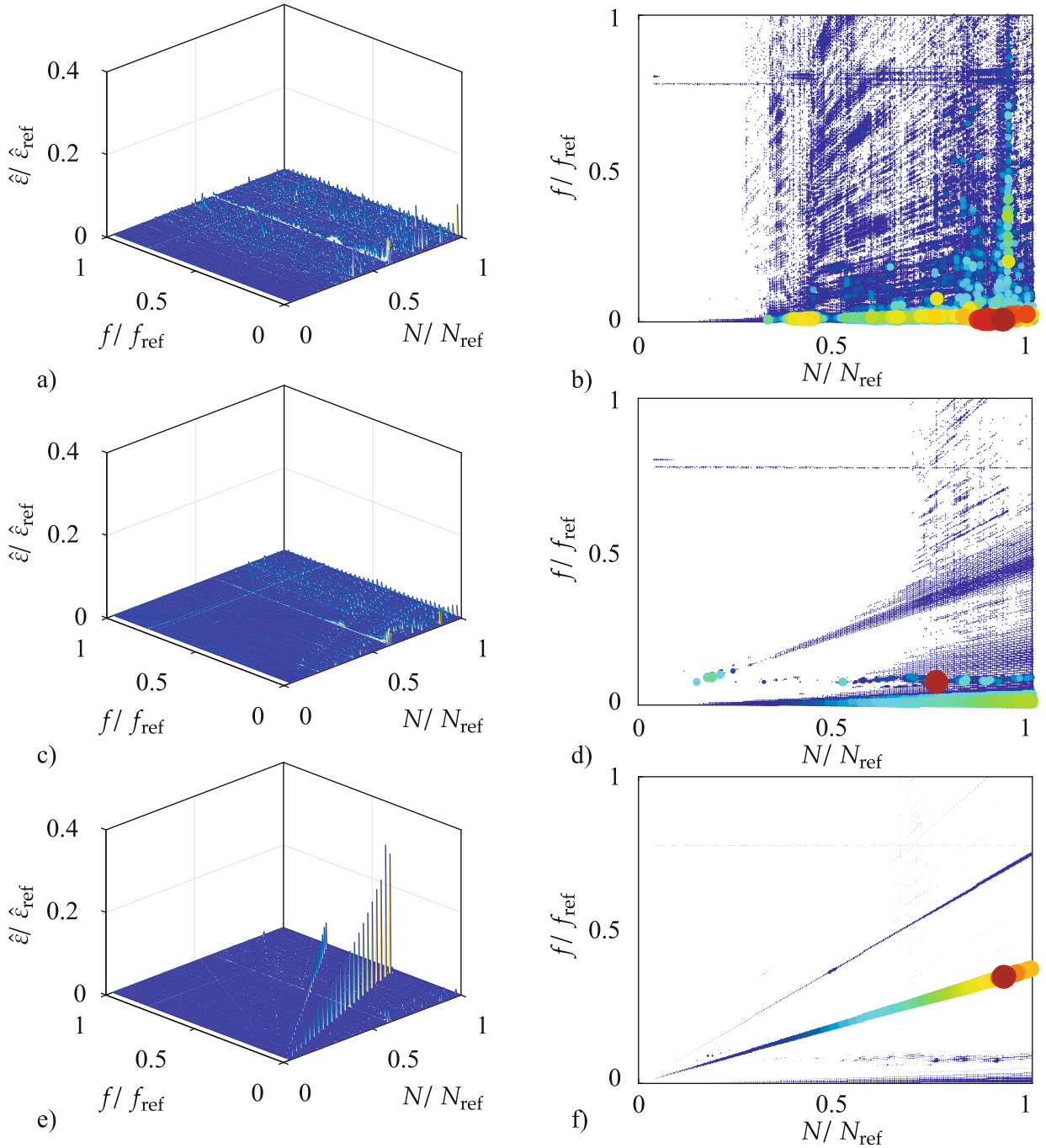

Fig. 21.5 Measured Campbell diagrams of the measurement sets 1–3: without magnet excitation (**a**, **b**), using one magnet (**c**, **d**), using 45 magnets (**e**, **f**)

of measurement set 3. For this purpose, the frequency responses along the first three orders, i.e. engine order (EO) 45 (red), 90 (blue) and 135 (green), are analyzed in detail, see Fig. 21.6a. The relation between the engine order EO and the nodal diameter ND is

$$EO = kN_{\mathrm{s}} \pm ND, \tag{21.1}$$

where N_{s} denotes the number of segments and $k = 0(1)\infty$. Thus, the nodal diameter 15 is excited by the engine order 45 and 135, and the nodal diameter 30 by the engine order 90. The frequency response of 5 repeated measurements is presented

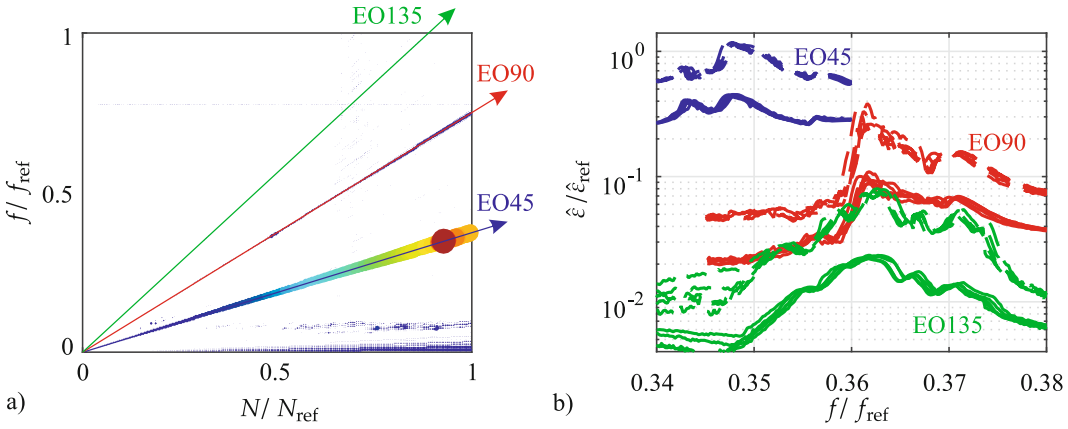

Fig. 21.6 Order analysis of measurement set 3 considering 5 repeated measurements: Campbell diagram with marked order numbers (**a**), mean (solid line) and maximum (dashed line) value of the vibration response at the orders 45, 90 and 135 (**b**)

in Fig. 21.6b, whereby the solid line represents the mean value and the dashed line the maximum value of all strain gauges. The obtained results are characterized by an excellent reproducibility as well as a high accuracy. The measured resonance frequencies at engine order excitation 45 and 90 clearly belong to the 1F-mode with nodal diameter 15 and 30, respectively. In particular, a resonance frequency shift of 5% between the engine order 45 and 135 is remarkable, even though it is theoretically the same mode shape , i.e. 1F-mode-ND15. This phenomenon is caused by the nonlinear structural mechanical behavior of the system and depends highly on the system's rotational speed. The rotational speed obtained by an engine order 45 excitation is three times larger as by an engine order 135 excitation. According to Fig. 21.2b, increasing the rotational speed leads—due to a change of the contact pressures at the joints—to lower natural frequencies.

In addition, the excitation level of the first harmonic, see Fig. 21.4d, is significantly larger than of the third harmonic leading to an additional frequency shift due to sliding processes at the joints. It is also noticeable that additional local maxima occur at engine order 135. This is caused by the gap mistuning of the excitation setup and the low energy input in this specific engine order. The nodal diameter 30 is excited by the engine order 90 (red lines) that corresponds to an antiphase mode shape of the blades. In this case, the resonance magnification shows an asymmetric, strongly nonlinear behavior. The unsteady curve progression implies local separation at the joints. Regarding the dynamic behavior of the whole system, it can be noted that the bladed disk model is highly mistuned. Due to manufacturing tolerances, material inhomogeneities and, in case of coupled bladed disks, installation conditions, the cyclic symmetry is highly disturbed leading to a mode and frequency splitting of the system, see [18]. As a result, the system's response consists of a superposition of standing and traveling waves despite a traveling wave excitation. With increasing the intensity of the mistuning, the amount of standing waves increases, while the travelling wave component decreases. Thus, localization effects can occur, such that some blades can show increased vibration amplitudes. This situation explains the differences between the maximum and the mean value in Fig. 21.6b.

To quantify the nonlinear structural mechanical effects, a gap variation and, thus, an excitation level variation is performed, see Fig. 21.7. It should be noted that for each gap value the mean value of 5 measurements is shown. For the sake of comparison, the results are normalized by a reference amplitude for each measurement set separately. Note that in the linear case, all frequency responses would lie on top of each other. Here, decreasing the gap between the magnets and blades leads to higher excitation forces and further to a decrease of the resonance frequencies. This is based on the frictional joints of the system. Increased excitation amplitudes lead to higher relative motion in the joints and, consequently, to more sliding and separation. In particular, the mode shapes of shrouded blades depend highly on the contact situation, as seen for instance in Fig. 21.2b. Regarding the 1F-ND15 mode, the maximum of the normalized response increases by increasing the excitation forces. This is obviously caused by a changing contact situation producing a slight change of the mode shape, see Fig. 21.7a. At off-resonance, the normalized response roughly shows a linear behavior. The 1F-ND30-mode shows a nonlinear jumping phenomenon, see Fig. 21.7b. An increase of the excitation level leads to lower frequencies and higher maximum amplitudes of the normalized vibration response. This is basically caused by the antiphase vibration between the blades with nodal diameter 30. Due to a high relative motion in normal direction of the shroud contact, local separation leads to a jumping phenomenon.

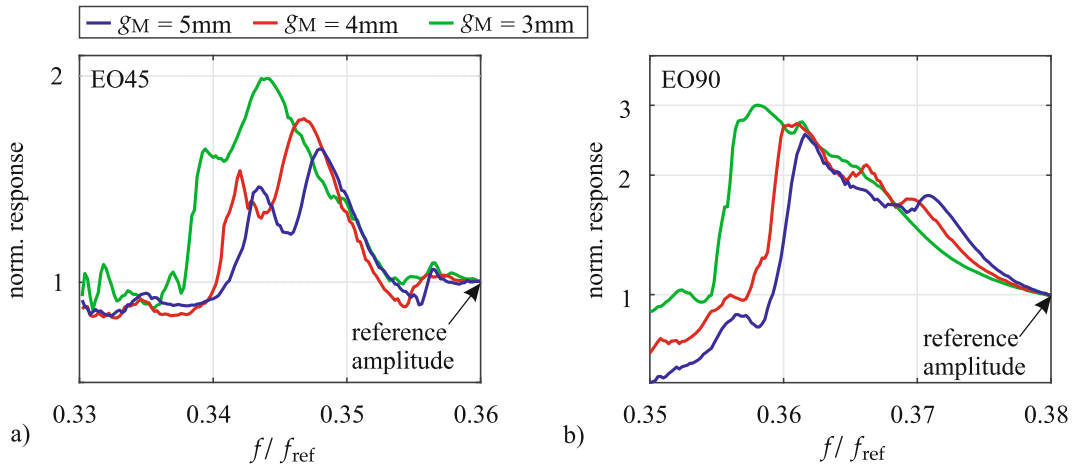

Fig. 21.7 Normalized vibration results by magnet gap variation: 1F-ND15-mode (**a**), 1F-ND30-mode (**b**)

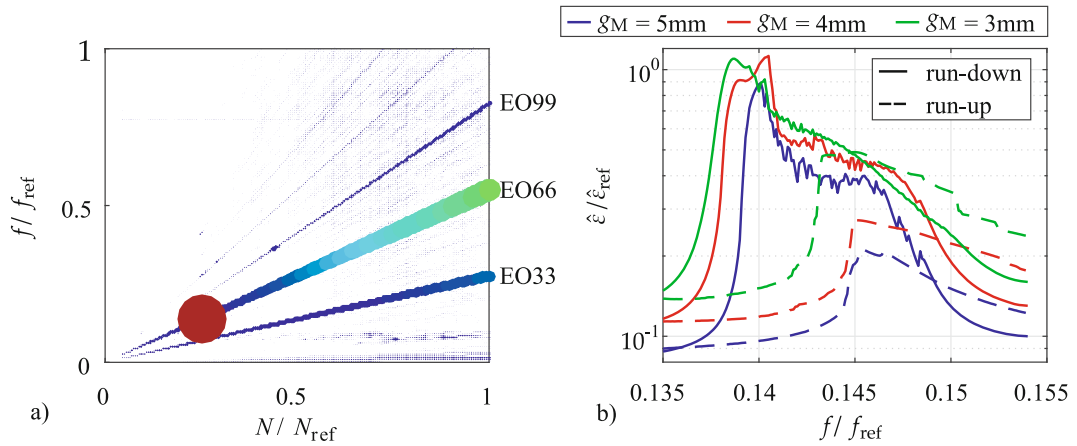

Fig. 21.8 Results of measurement sets 6–8: Campbell diagram (**a**), vibration results by an engine order 66 excitation (**b**)

In the last experimental study, the number of magnets is reduced to 33. According to Eq. (21.1), the nodal diameter 6 can be excited by the second harmonic of the excitation, i.e. EO66. In comparison to the nodal diameter 15, the nodal diameter 6 is isolated to other nodal diameters and is obviously a disk-dominated mode, see Fig. 21.2a. The Campbell diagram in Fig. 21.8a shows a resonance passage at the frequency $f/f\text{ref} \approx 0.14$ with the engine order 66. In addition, a resonance passage appears at the frequency $f/f\text{ref} \approx 0.37$ with the engine order 99, which corresponds to the nodal diameter 21. The amplitude level is comparatively low. Therefore, this mode is not considered further. Here, the order analysis is only applied to the engine order excitation 66, see Fig. 21.8b. Again, the mean value of 5 repeated measurements is considered. It is interesting to note that the vibration response shows significant differences between a run-up and a run-down measurement. A frequency difference of up to 4% can be noted. This phenomenon suggests that high contact separation occurs, which is, for instance, well-known for a prestressed mechanical gap oscillator. Due to high relative vibrations in normal direction of the contact, the contact separates leading to a spontaneous loss of stiffness and further to a reduction of the resonance frequency. The amplitude response is characterized by a hanging branch with multiple solutions at specific frequencies. The idealized model of a gap oscillator can be transferred only to a limited extent to the investigated bladed disk system. Due to the highly mistuned system, the contacts at the 60 blades do not separate simultaneously. Contact mistuning is still largely unexplored and should be investigated in future research to improve the understanding of shrouded bladed disks.

21.6 Conclusions

In this paper, a shrouded bladed disk model is investigated experimentally. A newly developed rotating test rig is used to measure the nonlinear vibration response for various excitation levels and engine orders. The developed excitation system, consisting of up to 45 permanent magnets, is analyzed in detail by means of a magnetostatic analysis and a validation of the excitation spectrum by an experimental test setup. The developed excitation system can be used to excite a specific engine order with a high energy input. It has been shown that the vibration response, i.e. resonance frequency as well as amplitude, strongly depends on the excitation and rotational speed level. In particular, the mode shapes of shrouded blades highly depend on the pressure distribution of the shroud contact. Increasing the excitation level leads to more local separation and, thus, to an increase of the vibration response at resonance condition. It could be noted that the system is highly mistuned, which, in this case, is mainly induced by the installation conditions leading to different contact pressures at the shrouds. Future work will be the numerical validation of the experimental results based on the computational methodology described in [15].

Acknowledgements The investigations were conducted as a part of the joint research program COOREFlex-turbo in the frame of AG Turbo. The work was supported by the Bundesministerium für Wirtschaft und Technologie (BMWi) as per resolution of the German Federal Parliament under grant number 03ET7020K. The authors gratefully acknowledge AG Turbo and MAN Energy Solutions SE for their support and permission to publish this paper. The responsibility for the content lies solely with its authors.

References

1. Petrov, E.P., Ewins, D.J.: Analytical formulation of friction interface elements for analysis on nonlinear multi-harmonic vibrations of bladed discs discs. In: Proceedings of ASME Turbo Expo 2002. American Society of Mechanical Engineers, New York (2002)
2. Siewert, C., Panning-von Scheidt, L., Wallaschek, J., Richter, C.: Multiharmonic forced response analysis of a turbine blading coupled by nonlinear contact forces. In: Proceedings of ASME Turbo Expo (2009)
3. Sever, I.A., Petrov, E.P., Ewins, D.J.: Experimental and numerical investigation of rotating bladed disk forced response using underplatform friction dampers. J. Eng. Gas Turbines Power **130**(4), 042503 (2008)
4. Firrone, C.M., T. Berruti.: An electromagnetic system for the non-contact excitation of bladed disks. Exp. Mech. **52**(5), 447–459 (2012)
5. Chang, J.Y., Wickert J.A.: Measurement and analysis of modulated doublet mode response in mock bladed disks. J. Sound Vib. **250**(3), 379–400 (2002)
6. Kielb, J.J., Abhari, R.S.: Experimental study of aerodynamic and structural damping in a full-scale rotating turbine. In: Proceedings of ASME Turbo Expo (2001)
7. Judge, J., Pierre, C., Mehmed, O.: Experimental investigation of mode localization and forced response amplitude magnification for a mistuned bladed disk. In: Proceedings of ASME Turbo Expo (2000)
8. Szwedowicz, J., Gibert, C., Sommer, T.P., Kellerer, R.: Numerical and experimental damping assessment of a thin-walled friction damper in the rotating setup with high pressure turbine blades. J. Eng. Gas Turbines Power **130**(1), 012502 (2006)
9. Gibert, C., Kharyton, V., Thouverez, F., Jean, P.: On forced response of a rotating integrally bladed disk: predictions and experiments. In: Proceedings of ASME Turbo Expo (2010)
10. Wildheim, S.J.: Excitation of rotationally periodic structures. J. Appl. Mech. **46**(4), 878–882 (1979)
11. Kammerer, A., Abhari, R.S.: Experimental study on impeller blade vibration during resonance–part II: blade damping. J. Eng. Gas Turbines Power **131**(2), 022509 (2009)
12. Szwedowicz, J., Sextro, W., Visser, R., Masserey, P.A.: On forced vibration of shrouded turbine blades. In: Proceedings of ASME Turbo Expo (2003)
13. Laxalde, D., Gibert, C., Thouverez, F.: Experimental and numerical investigations of friction rings damping of blisks. In: Proceedings of ASME Turbo Expo (2008)
14. Charleux, D., Gibert, C., Thouverez, F., Dupeux, J.: Numerical and experimental study of friction damping blade attachments of rotating bladed disks. Int. J. Rotating Mach. (2006). http://dx.doi.org/10.1155/IJRM/2006/71302
15. Kaptan, F., Panning-von Scheidt, L., Wallaschek, J.: Numerical and experimental study of shrouded blade dynamics considering variable operating points. In: ASME Turbo Expo 2018: Turbomachinery Technical Conference and Exposition. American Society of Mechanical Engineers, New York (2018)
16. Thomas, D.L.: Dynamics of rotationally periodic structures. Int. J. Numer. Methods Eng. **14**, 81–102 (1979)
17. Kenyon, J.A., Griffin, J.H., Kim, N.E.: Sensitivity of tuned bladed disk response to frequency veering. In: ASME Turbo Expo 2004: Power for Land, Sea, and Air. American Society of Mechanical Engineers, New York (2004)
18. Castanier, M.P., Pierre, C.: Modeling and analysis of mistuned bladed disk vibration: current status and emerging directions. J. Propul. Power **22**(2), 384–396 (2006)